Pergamon

Bioorganic & Medicinal Chemistry 7 (1999) 1683–1693

BIOORGANIC & MEDICINAL CHEMISTRY

A Reversible Monoamine Oxidase A Inhibitor, Befloxatone: Structural Approach of its Mechanism of Action

Johan Wouters,[a,*] Florence Moureau,[a] Guy Evrard,[a] Jean-Jacques Koenig,[b] Samir Jegham,[b] Pascal George[b] and François Durant[a]

[a]*Facultés Universitaires Notre-Dame de la Paix, rue de Bruxelles 61, B5000 Namur, Belgium*
[b]*Synthélabo Recherche, rue des Carriéres 10-BP 248, F92504 Rueil-Malmaison Cedex, France*

Received 23 June 1998; accepted 22 March 1999

Abstract—Experimental and theoretical physico-chemical methods were used to investigate the interaction between several reversible monoamine oxidase A inhibitors in the oxazolidinone series and the active site of the enzyme. Phenyloxazolidinones include toloxatone and analogues, among which befloxatone was selected as drug candidate for the treatment of depression. Identification of the forces responsible for the crystal cohesion of befloxatone reveals functional groups that could interact with monoamine oxidase. Calculation of electronic properties of those compounds using ab initio molecular orbital methods lead to a description of the mode of interaction between befloxatone and the cofactor of the enzyme. Electronic absorption spectroscopy measurements confirm the hypothesis of a privileged interaction of phenyloxazolidinone-type inhibitors with the flavin cofactor of MAO. Additional sites of interaction with the protein core of MAO A are also examined with regard to the primary structure of the enzyme. As a result of this work, a model is proposed for the reversible inhibition of MAO A by befloxatone via long distance, reversible interactions with the flavin adenine dinucleotide (FAD) cofactor of the enzyme and with specific amino acids of the active site. This model is partially corroborated by experimental evidence and should be helpful in designing new potent inhibitors of monoamine oxidase.

Introduction

Monoamine oxidase (MAO, EC 1.4.3.4) is a flavoenzyme located in the outer mitochondrial membrane responsible for oxidative deamination of many endogenous and exogenous monoamines. There are two major isoforms, MAO A and MAO B, distinguishable by their substrate specificity and their amino acid sequences.[1,2] Monoamine oxidase inhibitors (MAOIs) were the first class of drugs to be introduced for the treatment of depression. The irreversible nature as well as the non-specificity of those inhibitors are thought to be associated with their unfavorable side effect profile.[3]

Over the past few years, efforts have been directed to the design, synthesis and study of new reversible and selective MAOIs leading to compounds such as toloxatone,[4] moclobemide,[5] brofaromine,[6] and more recently befloxatone[7,8] (Fig. 1). Those compounds and others[4] block selectively MAO A[2] and do not form a covalent bond with the MAO enzyme,[3] they are acting via a reversible and competitive inhibitory mechanism. These MAO A inhibitors retain antidepressant effects in animal models and are devoid of severe food and drug incompatibilities induced by first generation MAOIs.

Toloxatone and befloxatone, belonging to the phenyloxazolidinone chemical family, structurally differ from the other MAOIs by the absence of an amino function. Indeed, this particularity is essential for reversibility as it has been shown by mechanistic studies that irreversible inhibitors generate reactive species trapped by MAO via strong covalent bonding with the enzyme.[9–11]

In order to explain the reversibility of these new generation inhibitors, a program was engaged to elucidate their mechanism of action at the molecular level, as a confirmation of previous studies.[12–16]

In this paper, we first discuss the molecular structure of befloxatone and some analogues as deduced from X-ray diffraction of monocrystals, in order to identify the forces responsible for the crystal cohesion. This structural approach is completed by conformational scanning allowing evaluation of torsions around the freely rotating bonds of the lateral butoxy chain of befloxatone in order to evaluate the flexibility of this moiety with

Key words: Enzyme inhibitors; X-ray crystal structures; monoamine oxidase; befloxatone.
* Corresponding author. Tel.: +32-81-724569; fax: +32-81-724530; e-mail: wouters@scf.fundp.ac.be

0968-0896/99/$ - see front matter
PII: S0968-0896(99)00102-9

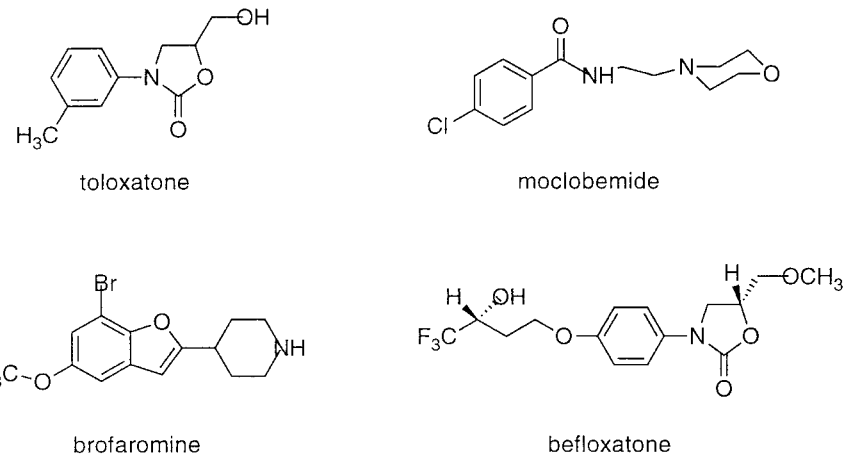

Figure 1. Chemical structure of the main reversible MAO A inhibitors.

regard to the steric hindrance of the active site and position the trifluorohydroxyl group interacting with the receptor. Then, the electronic properties of the molecule, i.e. electron densities, molecular electrostatic potential (MEP), atomic charges, delocalization effects, and charge transfer are computed by ab initio molecular orbital (MO) calculations. Electronic absorption spectroscopy of phenyloxazolidinone analogues of befloxatone and riboflavin confirm the possibility of a privileged interaction of befloxatone with the flavin cofactor of monoamine oxidase. These arguments suggest that this reversible inhibitor of MAO A interacts with the flavin adenine dinucleotide (FAD) cofactor of the enzyme through reversible, long distance interactions as have been determined for other molecules with related properties.[12–16]

Additional sites of interaction with the protein core of MAO A revealed by the structure–activity relationships have also been examined with regard to the primary structure of the enzyme. The possibility of a specific interaction of the trifluorohydroxyl group with a histidine residue of MAO A in a hydrophobic pocket, was examined using statistical analysis of the primary sequence of the enzyme, combined with the determination of the molecular lipophilic potential (MLP) of befloxatone.

As a result of this work, a model is proposed for the reversible inhibition of MAO by befloxatone via (i) long distance, reversible interactions with the FAD cofactor of the enzyme and (ii) intermolecular hydrogen bonds with specific amino acids in a hydrophobic pocket of the active site. The fact that befloxatone is engaged in a molecular association with MAO A through a double attachment at a primary and a secondary binding site could explain the great affinity and potency of this compound.

Results and Discussion

The CNS Medicinal Chemistry Department of Synthélabo Recherche synthesized befloxatone and the phenyloxazolidinones discussed in this paper. The synthesis of these molecules and their biological properties have been described.[4,7,8]

Restricted structure–affinity relationships among this series of compounds are summarized in Table 1 and Figure 2. The influence of the nature and length of the lateral alkoxy chain as well as the stereochemical requirements are illustrated for several analogues of befloxatone with respect to the inhibition of MAO A and MAO B.

Table 1. Main structure affinity results for the phenyloxazolidinone series. The affinity is expressed in terms of K_i for the two forms A and B of MAO

R	R′	Configuration at position 4	K_i A (nM)	K_i B (nM)
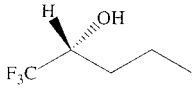	CH_3	R	2.5	222
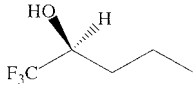	CH_3	R	28	16
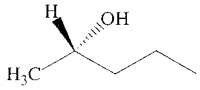	CH_3	R	6.1	1460
	CH_3	R	9.3	31
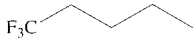	CH_3	R	2.4	4
CH_3	CH_3	R	130	769
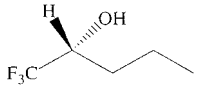	H	R	13	9.2
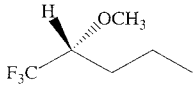	CH_3	R	53	2

X-ray structural analysis

A complete X-ray three-dimensional structure analysis of several phenyloxazolidin-2-one derivatives (Fig. 3) was performed in order to determine the main structural parameters, which might confer biological activity to befloxatone. Our discussion will be based on the search for common structural features able to explain the affinity of those compounds for MAO A.

Atomic numbering follows the one adopted in Table 4. A detailed description of the crystallographic parameters and experimental conditions of the structural study of molecules **I**, **II**, and **V** have already been presented.[17,18] The main structural features of compound **III** and **IV** are given in Table 2. A representation of their molecular structures is given in Figure 4 as an ORTEP plot.[19] Compound **IV** (the racemic mixture of **III**) crystallizes with two independent molecules in the asymmetric unit. Bond lengths, valence and torsion angles defining the structures are given in Tables 3 and 4.

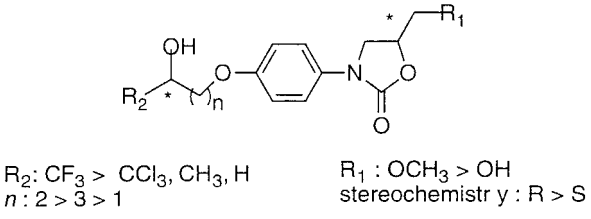

Figure 2. Structure-affinity relationships for selected phenyloxazolidinones.

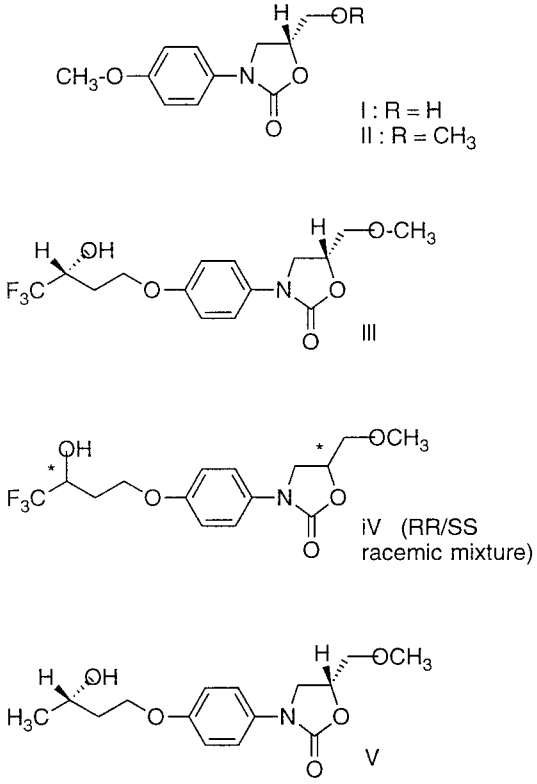

Figure 3. Chemical structure of befloxatone and some of its analogues. The atomic numbering adopted for oxazolidinones is given in Table 4.

The discussion of the molecular conformation, especially the spatial position of the essential hydroxyl group in befloxatone and the relative orientation of the phenyl and oxazolidinone rings, is based on the selected torsion angles given in Table 4.

Geometry of the phenyloxazolidinone moiety

The C(2)–N(8) and C(2)–O(3) bonds (Table 3) are always shorter than standard C_{sp3}–N and C_{sp3}–O bonds (1.469(10) Å and 1.432(13) Å, respectively) indicating electronic delocalization along N(8)–C(2)–O(3). The nitrogen atom N(8) presents an sp2 hybridization as the sum of the valence angles around this atom is close to 360° (Table 3).

Table 2. Main crystallographic data concerning compounds **III** and **IV**

III	**IV**
Crystal data	
$C_{15}H_{18}NO_5F_3$	$C_{15}H_{18}NO_5F_3$
$Mw = 349.3$	$Mw = 349.3$
Prisms	Colorless prisms
0.22×0.22×10 mm	0.29×0.25×0.24 mm
Monclinic	Monclinic
$P2_1$	$P2_1$
$a = 13.591(1)$ Å	$a = 18.668(3)$ Å
$b = 13.003(1)$ Å	$b = 8.879(2)$ Å
$c = 19.519(1)$ Å	$c = 10.226(1)$ Å
$\beta = 100.94(5)°$	$\beta = 102.69(1)°$
$V = 1652.1$ Å^3	$V = 1653.6$ Å^3
$Z = 2$	$Z = 4$
Density = 1.40 mg m^{-3}	Density = 1.40 mg m^{-3}
$F(000) = 728$	$F(000) = 728$
$\mu = 0.99$	$\mu = 0.84$
$T = 298$ K	$T = 298$ K
Data collection	
$\lambda = 1.54179$ Å (Cu K_α)	$\lambda = 0.71073$ Å (Mo K_α)
$\theta_{max} = 72°$	$\theta_{max} = 26°$
$\omega/2\theta$ scan	ω/θ scan
4501 independent reflections	3015 independent reflections
3012 reflections ($I > 2.5\sigma$)	1302 reflections ($I > 2.5\sigma$)
Refinement	
$R(F) = 0.039$	*$R(F) = 0.077$*
$wR(F) = 0.103$	$wR(F) = 0.209$
$S = 0.98$	$S = 1.07$
$(\Delta/\sigma)_{max} = 0.028$	$(\Delta/\sigma)_{max} = 0.001$
$\Delta\rho_{min}$[e/Å$_3$] = −0.22	$\Delta\rho_{min}$[e/Å^3] = −0.35
$\Delta\rho_{max}$[e/Å^3] = 0.16	$\Delta\rho_{max}$[e/Å^3] = 0.56

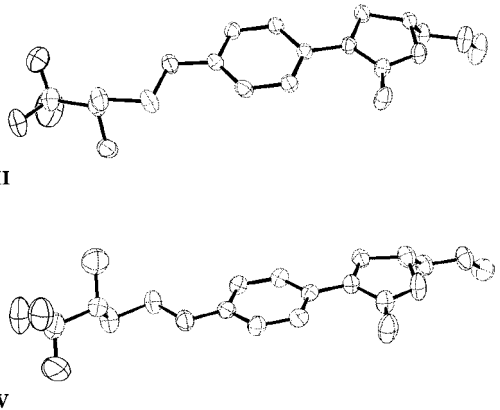

Figure 4. Molecular structure (ORTEP[19] view) of molecules **III** and **IV**.

The oxazolidinone ring is almost planar in all the molecules studied. For befloxatone, the maximal deviation from the mean plane containing the atoms C(2), O(3), C(4), C(7), N(8) is −0.018(2) and −0.029(3) Å for the carbon C(4), for the two molecules in the asymmetric unit, respectively.

This oxazolidinone ring is also coplanar with the adjacent phenyl ring as deduced from the C(2)–N(8)–C(9)–C(10) torsion angle close to 180° (Table 4). A conformational analysis (ab initio, RHF-LCAO-MO-SCF) performed on toloxatone and 5(*R*)-methoxymethyl-3-((4-methoxy)-phenyl)-oxazolidin-2-one (**II**) around the C(9)–N(8) bond reveals that the coplanarity between the oxazolidinone ring and the phenyl (C(9)–N(8) = 0 or 180°) corresponds to an energetically stable situation.[12,16]

Table 3. Selected bond lengths (Å) and valence angles (°) observed in the crystal structures of **I**–**V** for the common phenyloxazolidinone moiety

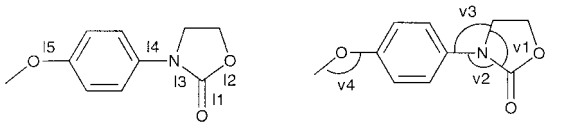

	I	II	III		IV	V
I1 (A)	1.218	1.187	1.219	1.212	1.199	1.202
I2 (A)	1.344	1.345	1.354	1.347	1.354	1.362
I3 (A)	1.340	1.368	1.353	1.360	1.350	1.365
I4 (A)	1.423	1.417	1.427	1.427	1.421	1.410
I5 (A)	1.372	1.361	1.375	1.381	1.372	1.374
v1 (°)	111.7	111.2	112.5	112.1	111.7	112.1
v2 (°)	126.1	126.0	125.9	126.1	126.1	125.0
v3 (°)	121.8	122.5	121.6	121.9	121.7	122.7
v4 (°)	117.5	118.0	115.5	117.2	117.9	118.9
V[a] (°)	359.6	359.7	360.0	360.1	359.5	359.8

[a] V = v1 + v2 + v3.

Stability of this planar geometry may result from conjugation between the two rings and/or formation of a intramolecular pseudo-hydrogen bridge involving O(1) and C(14) as observed in the crystalline state (e.g. O(1) ···C(14) = 2.867(7) Å in structure **II**).

The lateral 5(*R*)-methoxymethyl chain adopts two stable eclipsed conformations with a O(3)–C(4)–C(5)–O(6) torsion angle (Table 4) of +60° or −60°.

Conformation of the lateral chain

In all the alkoxyphenyloxazolidinone derivatives studied, the O(15) oxygen atom is sp^2 hybridized, the C(12)–O(15)–C(16) (v4 in Table 3) being close to 120° and the C(12)–O(15) bond length being around 1.37 Å. The C(11)–C(12)–O(15)–C(16) torsion angle is close to 0 or 180° and thus prolong the planar delocalized phenyloxazolidinone entity. For befloxatone, the lateral trifluorobutoxy chain adopts an extended *ttg* conformation: *trans* for C(17)–(C(11)–C(12)–O(15)–C(16) and C(12)–O(15)–C(16)–C(17) (torsion angles close to 0 and 180°) and *gauche* (g+) for C(17)–C(18) (O(15)–C(16)–C(17)–C(12) (torsion angle around +60°, Table 4). In order to determine a (bio)active conformation for this molecule, it is important to determine whether this conformation results from special packing constraints. This point will be discussed in the next part of this work. It is interesting to note that structures **III** (befloxatone) and **IV** adopt similar conformations although in different molecular environments. In fact, they only differ by the value (180 or 0°) of the torsion angle around C(16)–O(15) (Table 4). This difference, however greatly affects the relative positions of the OH and CF_3 groups versus the phenyloxazolidinone part of the molecule and will be taken into account when establishing a pharmacophore for this family of MAO A inhibitors.

Table 4. Selected torsion angles among substituted phenyloxazolidinones. The numbering scheme is presented[a]

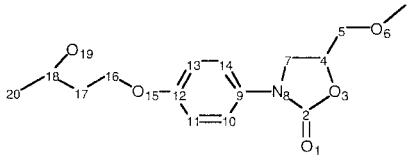

Torsion angles (°)	I	II	5-(*R*) toxatone	
C(2)–O(3)–C(4)–C(5)	−114.1 (2)	−119.0 (6)	−118.4 (2)	
O(3)–C(4)–C(5)–O(6)	63.2 (3)	61.5 (7)	67.3 (2)	
C(2)–N(8)–C(9)–C(14)	−13.9 (4)	17.4 (9)	2.4 (3)	
C(2)–N(8)–C(9)–C(10)	167.6 (2)	−165.2 (6)	−177.2 (2)	
C(11)–C(12)–O(15)–C(16)	2.5 (4)	−1.5 (9)	–	
Torsion angles (°)	**III** *Mol 100*	**III** *Mol 200*	**IV**	**V**
C(2)–O(3)–C(4)–C(5)	−117.9 (2)	−117.8 (2)	−129.3 (5)	−130.9 (3)
O(3)–C(4)–C(5)–O(6)	−63 (2)	60.0 (3)	−70.9 (6)	60.1 (3)
C(2)–N(8)–C(9)–C(10)	−179.6 (2)	161.3 (2)	−169.0 (5)	−168.7 (3)
C(7)–N(8)–C(9)–C(10)	−1.6 (2)	−16.9 (2)	1.9 (6)	5.4 (4)
C(11)–C(12)–O(15)–C(16)	170.2 (16)	−171.0 (2)	−4.9 (7)	174.8 (3)
C(12)–O(15)–C(16)–C(17)	−169.2 (2)	170.7 (2)	−179.5 (4)	−172.2 (3)
O(15)–C(16)–C(17)–C(18)	68.8 (3)	67.2 (4)	64.1 (6)	−169.2 (2)
C(16)–C(17)–C(18)–O(19)	67.3 (2)	68.0 (4)	60.2 (6)	−56.7 (3)
C(16)–C(17)–C(18)–C(20)	−172.2 (3)	−174.9 (3)	−177.8 (5)	−178.4 (3)

[a] *Mol 100* and *Mol 200* stand for molecule one and molecule two, respectively, in the asymmetric unit.

The analogue of befloxatone for which the CF_3 group is substituted by a methyl group (**V**) adopts an all *trans* conformation (Table 4).

Crystal packing

Analysis of the crystal packing of befloxatone shows that important π–π type interactions between the phenyl rings stabilize the structure in its solid state (Fig. 5). The coplanarity of the phenyl oxazolidinone moiety of the molecules allows optimal van der Waals interactions. The mean distances, ca. 3.5 Å, between two molecules parallely stacked (Fig. 5a) are shorter than the sum of the van der Waals (vdW) radii, 3.70 Å, obtained by the sum of the vdW radii of two phenyl carbon atoms. The stability of such observed dimeric structures (Fig. 5b) results mainly from π-type interactions and is increased by the presence of intermolecular hydrogen bonds: the lateral trifluorobutoxy chain of one molecule folds up to form an intermolecular hydrogen bond between the hydroxyl group of one molecule and the carbonyl of the oxazolidinone moiety of another. The crystal packing analysis for the analogues of befloxatone confirms the role played by the lateral chain in terms of intermolecular interactions and overall packing cohesion. The main intermolecular hydrogen bonds are listed in Table 5.

This brief overview of the forces responsible for the crystal cohesion clearly reveals the functional groups of befloxatone (and its analogues) that could be involved during interaction with another molecule, in particular the phenyloxazolidinone moiety of the molecule that could interact through π–π type van der Waals forces, the carbonyl oxygen (O1) and the hydroxyl group of the lateral chain which could participate in intermolecular hydrogen bonds.

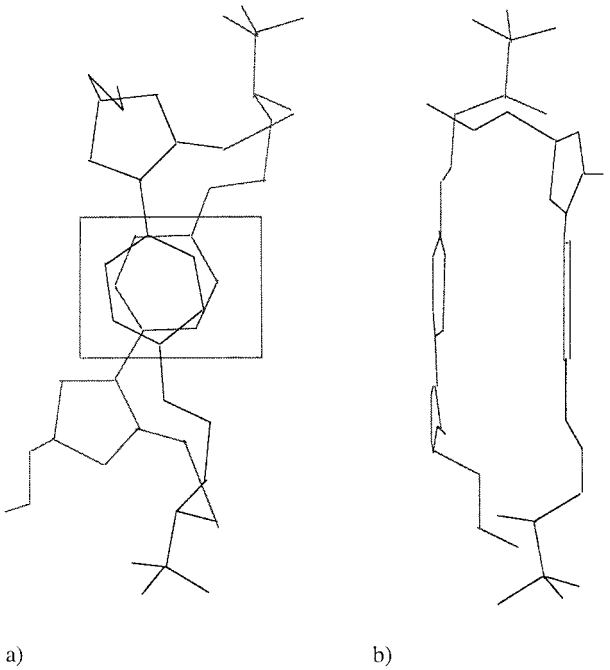

Figure 5. Crystal packing and molecular conformational in the structure of befloxatone (**III**). Dimeric structure viewed parallel (a) and perpendicular (b) to the planar phenyloxazolidinone moiety.

Theoretical conformational analysis

The molecular geometry obtained by X-ray diffraction might not correspond to the only stable conformation of a molecule. In order to evaluate the flexibility of the lateral chain of befloxatone and position the trifluorohydroxyl group with respect to the planar phenyl oxazolidinone moiety, the conformational space obtained by torsions around the freely rotating bonds of this lateral chain has been investigated using the semi-empirical MO AM1 method. The rigid rotor approximation can be applied in this case since C(16)–C(17) and C(17)–C(18) are single bonds. This analysis (Fig. 6) may help to position the essential groups of befloxatone into the enzyme pocket and gives insight into the steric hindrance at the active site of monoamine oxidase A. The 2-D iso-energy map displays successive contours with an interval of 0.5 kcal/mol. The zone where the energy is greater than 10 kcal/mol corresponds to forbidden conformations. The geometry observed in the crystalline state corresponds to low energy conformations.

Depending on the substitution, the lateral chain possesses more or less conformational freedom.[20] As a general rule, two forbidden areas appear at $T1 = 0°$, $T2 = 0°$ and/or $T1 = 120°$, $T2 = 0°$. They correspond to conformations for which steric interactions are strong and as a consequence, they have little chance to exist in the active site of the protein. Among the conformers studied, only the *trans* ($T1 = 180°$) $g+$ ($T2 = +60°$) is equally accessible to all the molecules. This geometry has been retained as 'consensus' conformation and selected for the modeling of the interaction with MAO A.

Compound **V** of Figure 3 (S configuration of the OH function of the butoxy chain) presents an all *trans* conformation for the lateral chain in the crystal state and does not adopt this 'consensus' conformation. However, superposition of the phenyloxazolidinone fragment of **III**, **IV**, and **V** allows the essential OH groups to occupy the same position in space.

Table 5. Main intermolecular hydrogen bonds among the substituted phenyloxazolidinones studied (**III**–**VII**)[a,b]

D-H...A	D...A (Å)	H...A (Å)	D-H...A (°)
III			
(19)–H(19)...O(1)*a*	2.748(4)	1.969	162.1
O(19)–H(19)...O(1)*b*	2.769(4)	1.755	173.4
IV			
O(19)–H(19)...O(6)*i*	2.758(7)	1.634	128.9
V			
O(19)–H(19)...O(19)*ii*	2.850(4)	2.080	174.0

[a] The numbering scheme is the same as in Table 2.
[b] The prefix *Mol 100* and *Mol 200* stand for molecule one and molecule two, respectively, in the asymmetric unit; a = *Mol 100*, b = *Mol 200*, $i = 1-x, -y, 1-z$, $ii = 1/2-x, 2-y, 1/2+z$.

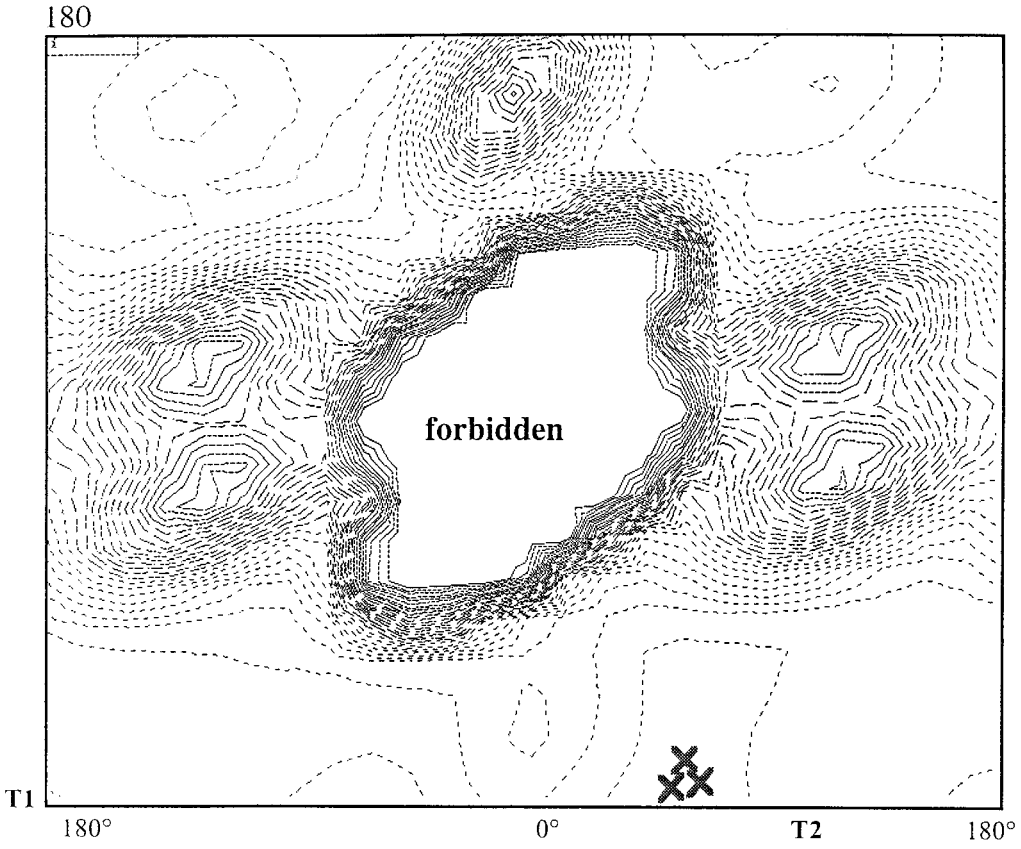

Figure 6. Conformational analysis (AM1) around the C(16)–C(17) (T1) and C(17)–C(18) (T2) bonds in befloxatone. The energy (kcal/mol) is determined for each conformer (15° steps for T1 and T2). In the isocontour map, allowed regions (from 0 to 10 kcal/mol, 0.5° kcal/mol steps) are presented by dashed lines and forbidden regions (> 10 kcal/mol) by solid lines. Conformations corresponding to the solid state structure are marked by a cross.

This structural information will be incorporated in a model of interaction with the binding site of monoamine oxidase A. Electronic (molecular orbital energy and topology, molecular electrostatic potential (MEP)) and lipophilicity properties (log k_w, molecular lipophilic potential (MLP)) of befloxatone are now analyzed in order to further investigate the interaction of reversible inhibitors of MAO A with the enzyme.

Electronic properties analysis

The importance of a planar electron rich moiety for MAO A reversible inhibition has been emphasized in previous studies of several families of molecules (phenyl oxazolidinones, β-carbolines, brofaromine, ...).[12–16] Calculation of electronic properties of those electron rich fragments suggested the possibility of a privileged interaction (charge transfer) of the inhibitors with the isoalloxazine ring of the flavin cofactor of MAO, which is also planar and known to be electron acceptor (Fig. 7). The strength of the molecular association is correlated with the energy of the HOMO (Highest Occupied Molecular Orbital) of the inhibitor: the better the electrons of the inhibitor can be transferred to the flavin, the stronger the interaction.[14] Like toloxatone and other reversible MAO A inhibitors, befloxatone contains a large planar electron-rich fragment that may engage a similar interaction with the flavin cofactor of the enzyme. This hypothesis is supported by the calculation, through ab initio MO methods of the electronic properties of flavin and befloxatone which clearly shows the possibility of overlap between the HOMO of the donor of electrons, befloxatone, and the Lowest Unoccupied Molecular Orbital (LUMO) of flavin.[16]

A priori, this interaction with the flavin should be better than in the case of toloxatone as the energy of the HOMO of befloxatone, −6.18 eV, is significantly less negative (i.e. it retains less electrons) than that of toloxatone, −6.40 eV.

At 1.75 Å above the phenyloxazolidinone plane, the molecular electrostatic potential (MEP) of befloxatone is similar to that of other reversible inhibitors of MAO A and is complementary with that of flavin, confirming our first interaction model.[12–14,20] The shape of the MEP calculated around befloxatone (Fig. 8) reveals modifications introduced by the 4,4,4-trifluoro-3(*R*)-hydroxy-butoxy chain on the electrostatic properties of phenyloxazolidinones. In addition to the attractive regions already present in toloxatone (−60 kcal/mol generated by the carbonyl oxygen O(1) and −45 kcal/mol for the intracyclic O(3) oxygen atom) a new attractive potential well (−25 kcal/mol) is induced by the hydroxyl function of the butoxy chain. An additional site of interaction is thus present there what was already implicit from the X-ray diffraction analysis (possibility of additional H bonds within the binding site of MAO).

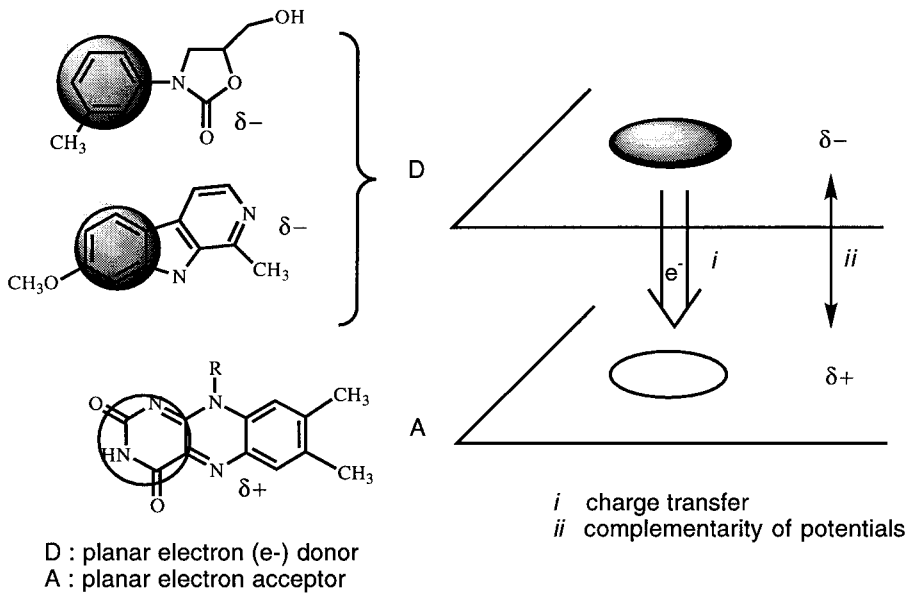

Figure 7. Model of reversible inhibition of MAO A.[12–16] The molecular association between the reversible inhibitors (D) like phenyloxazolidinones or β-carbolines and the flavin cofactor (A) results from (i) a net transfer of electrons (e^-, charge transfer between hashed surfaces) and (ii) the complementary of molecular electrostatic potentials (δ+ and δ−) generated by the two partners (A and D) of the complex.

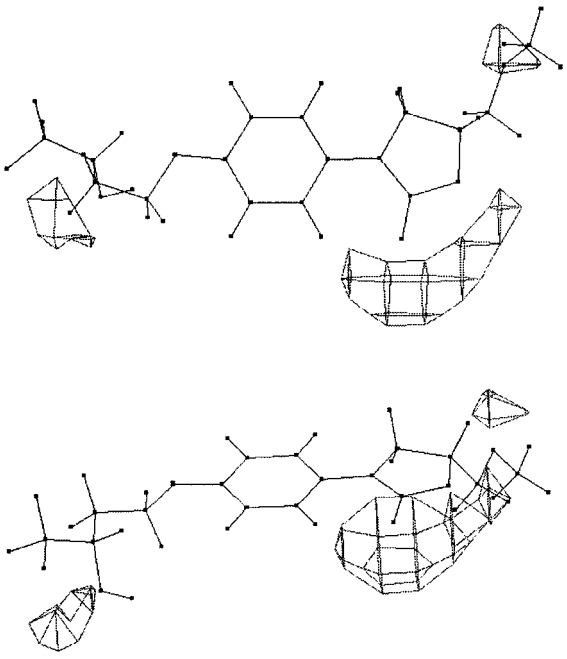

Figure 8. Molecular electrostatic potential (MEP) calculated around befloxatone. Two views at 90° are presented.

Analysis of lipophilicity

The measured (reverse-phase high pressure liquid chromatography, RP-HPLC) lipophilicity of befloxatone, expressed as log k_w is 2.45, which means that the molecule is hydrophobic. A detailed analysis of this property in a series of phenyloxazolidinones clearly revealed that the lipophilicity alone is not sufficient to explain the variations of affinity for MAO A.[21] Hydrophobicity however plays a major role in MAO B inhibition. Others have studied this point among different MAO ligands.[22,23] The molecular lipophilicity potential (MLP) is useful in that it reflects the anisotropy of the lipophilicity property of a molecule and reveals potential interaction sites between a ligand and its receptor. Computed on befloxatone, the MLP underlines the lipophilic character of the molecule, in agreement with the value of log k_w.[21] Two hydrophilic regions appear around befloxatone, the first generated by the two oxygen atoms of the oxazolidinone ring and the second corresponding to the OH group of the lateral trifluorobutoxy chain. Both regions of the inhibitor will correspond to polar residues in the receptor site of the enzyme.

Electronic absorption spectra

Complexation of riboflavin by different analogues of befloxatone is clearly demonstrated in solution and leads to a 1:1 charge transfer complex characterized by a new absorption band at 492 nm. The experimental protocol was the same as in previous studies.[12–15] Introduction of an alkoxy group on the phenyl ring of phenyloxazolidinones induce a redshift of the absorption band (λ_{max}) characteristic of the intermolecular electron transfer in the complex, as could be expected by the lower ionization potential of those molecules (vide supra energy of the HOMO).

Complexation constants (K_c) were deduced from a Foster–Hammick–Wardley plot[24,25] (data not shown). The fact that those constants are of the same order of magnitude for the three different butoxy substituted phenyl oxazolidinones and that they present the same value of λ_{max}, whatever the substitution, strongly suggests that only the phenyloxazolidinone part of the molecules is involved in complexation of the flavin ring. Moreover, in solution, introduction of this butoxy chain diminishes complexation (K_c is significantly smaller than

for toloxatone) and implicitly demonstrates the need of an additional anchoring site in the active site of MAO A in order to account for the better affinity for those compounds for the protein.

Analysis of the primary structure of monoamine oxidase

Monoamine oxidase (MAO, flavin containing amine oxidase, EC 1.4.3.4) occurs as two separate gene products, MAO A and MAO B, which share about 70% sequence homology as found by sequencing their respective cDNAs.[1,2] Both forms contain the FAD (flavin adenine dinucleotide) cofactor covalently bound to the protein via a thioether linkage to a cystein (Cys 406).[26] Statistical analysis of the primary sequence of monoamine oxidase (structure identity, physicochemical properties, hydrophobicity, Eisenberg analysis, HCA), determination of its secondary structure by IR spectroscopy[27] and comparison with the three dimensional structure of several flavoproteins[20] (glutation reductase, thioredoxin reductase, *p*-hydroxybenzoate hydroxylase) have been performed. And recent results come from mutagenesis studies.[28–33]

In addition to a primary binding site corresponding to the phenyloxazolidinone part of befloxatone (charge transfer interaction with the isoalloxazine ring of the FAD cofactor and hydrogen bonds between the oxazolidinone ring into the active site) it is reasonable to postulate additional stabilization by the protein with phenyloxazolidinone-type inhibitors. In particular, hydrogen bonds must help to stabilize the position of the OH group of the lateral butoxy chain. To be consistent with the specific biological profile of befloxatone, this interaction with MAO must involve an amino acid located in a region of the sequence responsible for the specificity of the protein. We postulate a specific interaction of this OH group with a histidine residue. Indeed, this residue is often implicated in hydrogen bonds at active sites of proteins and its amphoteric character may explain the fact that transformation of the hydroxyl group of befloxatone into a carbonyl function only slightly affects the affinity and specificity for MAO A.[7]

The preference for a histidine is also motivated by arguments found in the literature. In particular the crucial role played by this residue in MAO has been demonstrated by kinetic studies and chemical modification experiments,[34] His148 could be a good candidate. The choice of His148 comes from the analysis of the primary sequence of monoamine oxidase. This residue is the only histidine conserved among all known sequences of MAO A and specifically replaced by another residue in MAO B. His148 is also close to Cys165. This cysteine is essential for the activity of MAO as deduced from mutagenesis.[28]

The specific substitution of histidine 148 by a leucine in the sequences of MAO B may explain the more important role of lipophilicity for MAO B inhibition. Moreover His148 is located in a globally hydrophobic segment of the protein as deduced by hydrophobicity plots compatible with the MLP profile of befloxatone.

Interaction model

The diagram presented in Figure 9 illustrates the model of interaction between oxazolidinones and the FAD cofactor, including structural, electronic and hydrophobicity properties of those molecules. It incorporates results available for the protein (sequence analysis, mutagenesis results). This model illustrates our hypothesis of double attachment of befloxatone to MAO A and shows anchoring sites to the protein. These postulated enzyme-inhibitor interactions are reversible (charge transfer, hydrogen bonding) and agree well with the biological profile of the molecule. The improved inhibition of MAO A by befloxatone versus toloxatone is explained by the possibility of additional stabilization of the 4,4,4-trifluoro-3(*R*)-hydroxy-butoxy chain. Quantitative determination of the relative positions of the different elements defined in this model is possible thanks to the steric and electronic descriptors presented in this work.

Conclusion

Analysis of the forces responsible for the crystal cohesion clearly reveals the functional groups of befloxatone (and its analogues) which could interact with the MAO active site, in particular the phenyloxazolidinone moiety of the molecule which could interact through π–π type van der Waals forces and the hydroxyl group of the lateral chain which could participate in intermolecular hydrogen bonds. The importance of a planar electron rich moiety for MAO A inhibition has already been emphasized in previous reports for phenyloxazolidinones, including toloxatone, and reversible inhibitors belonging to other families.[12–14] The increased inhibitory potency observed with befloxatone compared to toloxatone can be attributed to additional specific interactions with the protein.

The structural characterization of the substituted phenyloxazolidinones has been completed by conformational calculations and quantitative steric descriptors have been deduced.

Calculation of the electronic properties (molecular orbital topologies and energies) of those compounds using ab initio molecular orbital methods led to a description of a primary interaction between befloxatone and the cofactor of the enzyme. Electronic absorption spectroscopy measurements confirmed the possibility of a privileged interaction of this inhibitor with the flavin cofactor of MAO.

Additional sites of interaction with the protein core of MAO A, revealed by structure–activity relationships, electronic (molecular electrostatic potential), and lipophilicity properties, were also examined with regard to the primary structure of the enzyme.

As a result of this work, a model is proposed (Fig. 9) for the reversible inhibition of MAO by phenyloxazolidinones via long distance, reversible interactions with the enzyme. It is assumed that befloxatone is engaged in a molecular association with MAO A

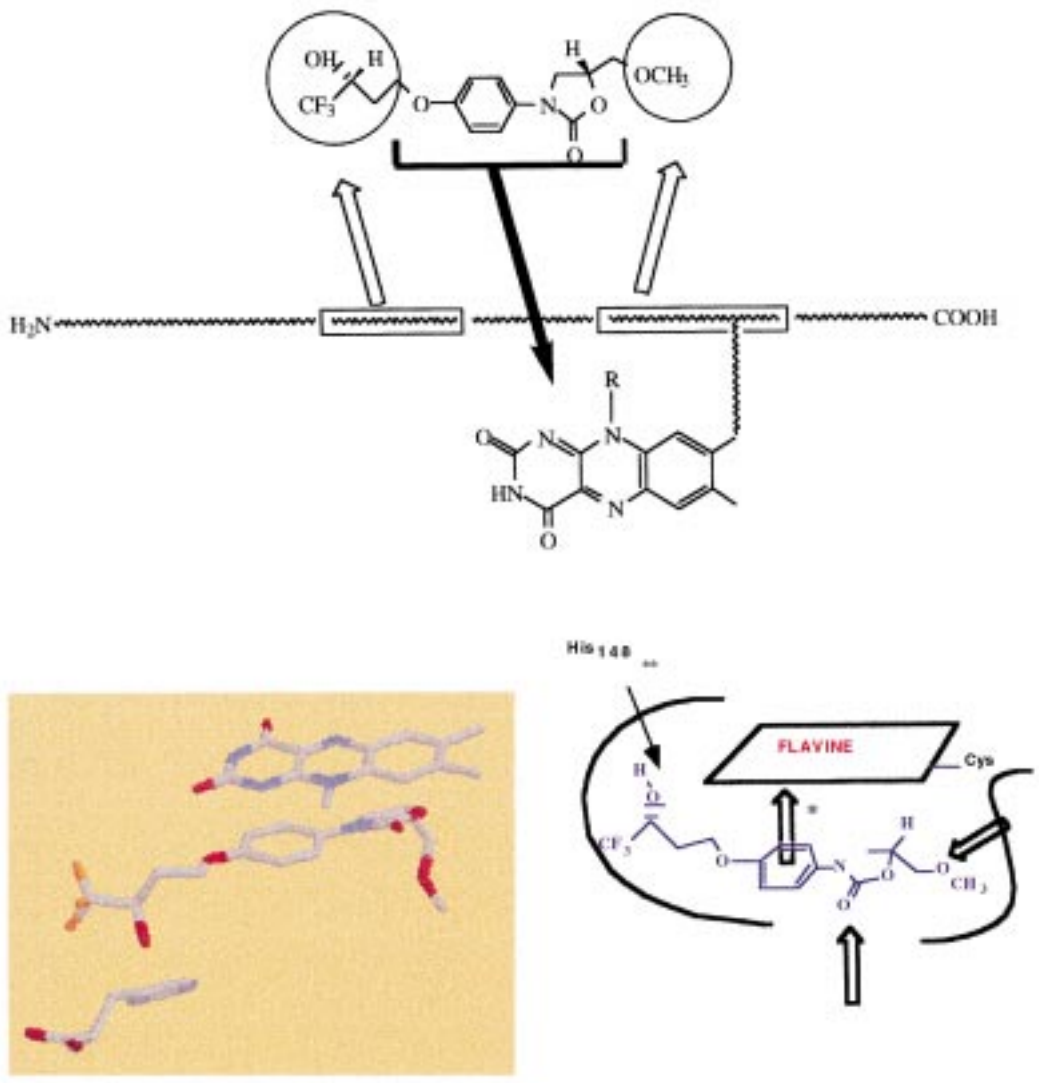

Figure 9. Proposed model of reversible inhibition of MAO A by befloxatone. *Stabilization of the phenyloxazolidinone (charge transfer interaction with the isoalloxazine ring of the flavin cofactor and hydrogen bonds involving the oxazolidinone ring) and **specific interaction of the lateral chain (stabilization of a hydroxyl by a histidine) within a hydrophobic pocket. The increased potency of befloxatone is explained by the possibility of additional interactions with the protein that are not possible for toloxatone.

through a double attachment at a primary and secondary binding site: (i) stabilization of the phenyloxazolidinone (charge transfer interaction with the isoalloxazine ring of the flavin cofactor and hydrogen bonds involving the oxazolidinone ring) and (ii) specific interaction of the lateral chain (stabilization of a hydroxyl by H bonding) within a hydrophobic pocket.

This model should be helpful in designing new potent reversible MAO A inhibitors.

Experimental

X-ray diffraction

Cell parameters were obtained by least-square refinement of 25, medium-angle reflections. Intensities collected on an Enraf–Nonius CAD-4 diffractometer were corrected for Lorentz and polarization effects. The structures were solved by direct methods using the SHELXS86 program.[35] The refinement was performed with SHELXL,[36] by full-matrix least-squares on F. The molecular geometry analysis was carried out with the X-ray program.[37,38] The stereoscopic view drawings of the molecular conformation and crystal packing were generated by the ORTEP program.[19]

Ab initio molecular orbital method

The molecular orbital topology, that is, pattern of the highest occupied molecular orbital (HOMO) and the lowest unoccupied molecular orbital (LUMO), and the electronic properties of befloxatone, that is, π-overlap populations, atomic charges, and molecular electrostatic orbitals (MEP) were obtained at the non-empirical Restricted Hartree-Fock (RHF) LCAO-MO-SCF (linear combination of atomic orbitals-molecular orbitals-self consistent field) level of electronic theory. At this level, one considers the independent motion of a single

electron in the electrostatic field of fixed nuclei and averaged Coulomb and exchange fields due to other electrons. This level of the theory results in the traditional molecular orbital (MO) language.

The atomic coordinates of the heavy atoms considered in our calculations are obtained by the crystallographic resolution of the structures of lumiflavin[20] and befloxatone; all H-atoms were located at standard positions (bond lengths, valence and torsion angles) from their carrier atoms. The generation of the electron charge density two-dimensional iso-contour maps was performed with the Moplot (Molecular Orbital Plot) subprogram[39] available within the Motecc (Modern Techniques in Computational Chemistry) package.[40] All computations were carried out using the Gaussian92 programs[41] adapted to a IBM Risc 6000 computer system. Exploring the conformational space was limited to allow rotation around the flexible single bonds of the lateral butoxy chain of befloxatone. The stability of the other moieties of the molecules was discussed elsewhere. Conformational calculations were performed using the semi-empirical quantum mechanical molecular orbital (MO) AM1 method developed by Dewar.[42] The good performance of this method for conformational analysis problems has been largely documented. Iso-contour energy maps were obtained by systematic variation of the torsion angles 1 and 2 (increment between two calculations: 15°) using the AM1 facilities with the parameters as available within the Gaussian.[41] The 2D iso-contour maps were drawn with an in-house device-independent contouring program CPS (Contouring Plotting System)[42] developed in Fortran with the IBM graPHIGS software.[40]

Electronic absorption spectroscopy

The spectrophotometric measurements were carried out with a UVIKON 930 (Kontron instruments) spectrophotometer and a thermostatic cell holder adapted for 1 cm cells. Circulating water maintained the holder at constant temperature. Glass cells of 1 cm pathlength were used. Spectra were recorded with the UVIKON 930 Scan program. The products were dissolved in a phosphate buffer (pH 6, ionic strength = 2×10^{-1} M). The concentrations of the different MAOIs ranged from 3.3×10^{-2} to 1.5×10^{-1} M depending on the solubility of the compounds. ((3-Amino butoxy) phenyl)-5-methoxymethyloxazolidin-2-one derivatives were used because they are more soluble than the corresponding hydroxyl substituted compounds. The concentration of riboflavin was maintained constant and of the order of 1.5×10^{-4}. The temperature range was 0–10° C.

Biochemistry

The in vitro MAO activity was measured in rat whole brain homogenates using [^{14}C]-5-HT (serotonin) as substrate for MAO_A or [^{14}C]-PEA (phenylethylamine) as substrate for MAO_B following a published procedure.[43]

Preparation of homogenates. Male Sprague–Dawley rats weighing 125–300 g were used. After sacrifice by decapitation, the brain was rapidly removed, weighed and homogenized in a buffer solution (Na_2HPO_4/NaH_2PO_4, 0.1 M, pH 7.4) at 4°C using an Ultra Turrax (or Polytron) homogenizer at maximum speed for 10 s. The composition of the homogenates was 1 g tissue/20 mL buffer.

Reaction mixture. MAO activity was measured in test-tubes containing 500 μL of a reaction mixture of the following composition: 100 μL homogenate, 100 μL substrate, 50 μL test compound (or 50 μL H_2O for controls and blanks), 250 μL buffer (qsp for 500 μL). The homogenate was preincubated 20 min at 37°C with the buffer, with or without (controls and blanks) the test compound and the reaction started by adding the substrate and incubating with stirring at 37°C for 5 min ([^{14}C]-5-HT, 65 μM) or 1 min ([^{14}C]-PEA, 40 μM).

Acidification and extraction of metabolites. The reaction was stopped by precipitating the proteins with 200 μL 4 N HCl and by placing the test-tubes in ice. Blanks were obtained by precipitating the proteins before adding the substrate. The metabolites formed were extracted with 7 mL of a (v/v) toluene/ethyl acetate mixture. The test-tubes were shaken 10–15 min, frozen, and 7 mL of the upper (organic) phase removed. This sample was shaken 5 min and the radioactivity counted by liquid scintillation in 8–10 mL of a toluene/2.5 diphenyloxazole mixture (4 g l−1).

Results. The mean values for controls and assays with test compound were calculated after subtraction of the mean values of the corresponding blanks. The percentages inhibition was calculated by comparing the mean values of assays with the test compound, with those of controls and the graphic representation of percentage inhibition versus concentration of the test compound gave the IC_{50} (concentration of test compound that reduces MAO activity by 50%) and corresponding K_i.

Acknowledgments

J.W. acknowledges the Belgian National Foundation for Scientific Research (FNRS) for his Research Assistant position. The authors thank the FNRS, IBM-Belgium, and the Facultes Universitaires Notre-Dame de la Paix for the use of the Namur Scientific Computing Facility, and Dr O. Curet for in vitro biochemical results.

References

1. Johnston, J. P. *Biochem. Pharmacol.* **1968**, *17*, 1285.
2. Weyler, W.; Hsu, Y. P.; Breakefield, O. *Pharmac. Ther.* **1990**, *47*, 391.
3. Brunello, N.; Langer, S.; Perez, J.; Racagani, G. *Depression* **1995**, *2*, 119.
4. Ferrey, G., Rovei, V., Strolin Benedetti, M., Gomeni, C., Languillat, J. M. In *Clinical and Pharmacological Studies in Psychiatric Disorders*; Burrows, G., Norman, T., Dennerstein, L., Eds. Libbey: Paris, 1985; pp 83–86.
5. Fulton, B.; Benfield, P. *Drugs* **1996**, *52*, 450.

6. Verhoeven, W. *Prog. Neuro-Psychopharmacol. Biol. Phychiat*. **1994**, *18*, 235.
7. Jarreau, F. X., Rovei, V., Koenig, J. J., Schoofs, A. 1989 French patent 2653017.
8. Curet, O.; Damoiseau, G.; Labaune, J.-P.; Rovei, V.; Jarreau, F. X. *J. Neural. Transm. Suppl* **1994**, *41*, 349.
9. Silverman, R.B. In *Advances in Electron Transfer Chemistry*; Mariano, P., Ed.; JAI: Greenwich, 1992; Vol. 2, pp 177–213.
10. Dostert, P.; Strolin Benedetti, M.; Tipton, K. *Med. Chem. Rev*. **1989**, *9*, 45.
11. Kalgutkar, A.; Castagnoli, N.; Testa, B. *Med. Chem. Rev*. **1995**, *15*, 325.
12. Moureau, F.; Wouters, J.; Vercauteren, D. P.; Collin, S.; Evrard, G.; Durant, F.; Ducrey, F.; Koenig, J. J.; Jarreau, F. X. *Eur. J. Med. Chem* **1992**, *27*, 939.
13. Moureau, F.; Wouters, J.; Vercauteren, D. P.; Collin, S.; Evrard, G.; Durant, F.; Ducrey, F.; Koenig, J. J.; Jarreau, F. X. *Eur. J. Med. Chem* **1994**, *29*, 269.
14. Moureau, F.; Wouters, J.; Vercauteren, D. P.; Depas, M.; Durant, F.; Ducrey, F.; Koenig, J. J.; Jarreau, F. X. *Eur. J. Med. Chem* **1995**, *30*, 823.
15. Wouters, J.; Moureau, F.; Vercauteren, D. P.; Evrard, G.; Durant, F.; Koenig, J. J.; Ducrey, F.; Jarreau, F. X. *J. Neural. Transm. Suppl*. **1994**, *41*, 313.
16. Wouters, J., Moureau, F., Dory, M., Evrard, G., Durant, F., Ducrey, F., Koenig, J. J., Jarreau, F. X. In *Trends in QSAR and Molecular Modelling 92*; Wermuth, C., Ed. ESCOM: Leiden, 1993; pp 291–293.
17. Wouters, J.; Perpete, P.; Norberg, B.; Evrard, G.; Durant, F. *Acta Cryst*. **1994**, *C50*, 97.
18. Wouters, J.; Evrard, G.; Durant, F. *Acta Cryst*. **1994**, *C50*, 1490.
19. Johnson, C. *Program ORTEP II, Oak Ridge Thermal Ellipsoid Plot*; Oak Ridge, TN, 1971.
20. Wouters, J. PhD thesis, 1995; Fac. Uni. ND de la Paix, Belgium.
21. Ooms, F.; Wouters, J.; Collin, S.; Gaillard, P.; Durant, F. *Bioorg. Med. Chem. Lett*. **1998**, *8*, 1425.
22. Kneubühler, S.; Thull, U.; Altomare, C.; Carta, V.; Gaillard, P.; Carrupt, P. A.; Carotti, A.; Testa, B. *J. Med. Chem*. **1995**, *38*, 3874.
23. Edmondson, D. *Biochimie* **1995**, *77*, 643.
24. Foster, R.; Hammick, D.; Wardley, A. *J. Chem. Soc*. **1953**, *IV*, 3817.
25. Foster, R. In *Charge Transfer Interactions of Biomolecules*; Academic: London, 1971.
26. Kearney, E.; Salach, J.; Walker, W.; Seng, R.; Kenney, W.; Zeszotek, E.; Singer, T. P. *Eur. J. Biochem*. **1971**, *24*, 321.
27. Wouters, J.; Ramsay, R.; Goormaghtigh, E.; Ruysschaert, J. M.; Brasseur, R.; Durant, F. *Biochem. Biophys. Res. Commun*. **1995**, *208*, 773.
28. Wu, H. S.; Chen, K.; Shih, J. *Mol. Pharmacol*. **1993**, *43*, 888.
29. Tsugeno, Y.; Hirashiki, I.; Ogata, F.; Ito, A. *J. Biochem*. **1995**, *118*, 974.
30. Grimsby, J.; Zentner, M.; Shih, J. *Life Sci*. **1996**, *58*, 777.
31. Zhou, B.; Lewis, D.; Kwan, S. W.; Kirksey, T.; Abell, C. *Biochem*. **1995**, *34*, 9526.
32. Kwan, S. W.; Lewis, D.; Zhou, B.; Abell, C. *Arch. Biochem. Biophys*. **1995**, *316*, 385.
33. Chen, K.; Wu, H. F.; Shih, J. *J. Neurochem*. **1996**, *66*, 797.
34. Hiramatsu, A.; Tsurushiin, S.; Yasunobu, K. *Eur. J. Biochem*. **1975**, *57*, 587.
35. Sheldrick, G. M. 1986 SHELXS86. A program for crystal structure determination. Institut für Anorganische Chemie der Universität, Göttingen, 1986.
36. Sheldrick, G. M. SHELX76. A program for crystal structure determination. University of Cambridge: Cambridge, 1976.
37. Steward, J. M., Machin, P. A., Dickinson, C. W., Ammon, H. L., Heck, M., Flack, H. X-ray, Technical report TR-445. Computer Science Center: University of Maryland, MD, 1976.
38. Hinde, R. J., Luken, W. L., Chin, S. IBM Kingston Technical report KGN-141: New York, 1988.
39. Chin, S., Vercauteren, D. P., Luken, W. L., Re, M., Scateni, R., Tagliavini, R., Vanderveken, D., Baudoux, G. In *Modern Techniques in Computational Chemistry: MOTECC 89*; Clementi, E., Ed. ESCOM: Leiden, 1989; pp 499–546.
40. Frish, M. J., Binkley, J. S., Schlegel, H. B., Raghavachari, K., Melius, C., Martin, R., Stewart, J. J., Bobrowicz, F., Rohlfing, C. M., Kahn, L. R., Defrees, D. J., Seeger, R., Whiteside, R., Fox, D. J., Fleuder, E. M., Pople, J. A. *Gaussian 86*; Canegie-Mellon Quantum Chemistry Publishing Unit: Pittsburgh, 1988.
41. Dewar, M.; Zoebisch, E.; Healy, F.; Stewart, J. J. *J. Am. Chem. Soc*. **1985**, *105*, 3902.
42. Baudoux, G., Vercauteren, D. P. *CPS, a Contour Plotting System*; Facultés Universitaire Notre-Dame de la Paix, 1989.
43. Fowler, C.; Strolin-Beneditti, M. *J. Neurochem*. **1983**, *40*, 1534.